Recognition of Osteoporosis Based on Texture Analysis and a Support Vector Machine

Jie Cai[1#], Tian-Xiu Wu[2#], Ke Zhou[1], Wende Li[3]*

[1]*School of Information Engineering*
Guangdong Medical College
E-mails: caijie513@163.com, kitty@gdmc.edu.cn

[2]*School of Basic Medical Science*
Guangdong Medical College
E-mail: wutianxiu2005@163.com

[3]*Key Laboratory of Natural Drug Research and Development of Guangdong*
Department of Pharmacology, Guangdong Medical College
2 Wengmingdong Road, Xiashan District, Zhanjiang City
Guangdong Province, China
E-mail: gdmcli@qq.com

[#]*Equally contributed*
[*]*Corresponding author*

Received: December 07, 2014 **Accepted: March 26, 2015**

Published: April 01, 2015

Abstract: *To explore a new approach for osteoporosis recognition with images, a texture analysis was made of 27 bone tissue images (16 of which from a SHAM group, and 11 from an OVX group). Texture features were then extracted through a co-occurrence matrix and a run-length matrix, and the texture features with significant differences between the two groups were chosen and used as the features in the classification course based on a Support Vector Machine (SVM). The results show that there are obvious statistic differences between the SHAM group and the OVX group in terms of texture features. Furthermore, the highest recognition accuracy was achieved at 92.59%. A SVM based on a linear function showed the highest accuracy rate and the lowest error rate in recognition. This new approach can be used to recognize osteoporosis effectively and thus can provide a valuable reference to the clinical application in osteoporosis diagnosis with medical images.*

Keywords: *Texture analysis, Support vector machine (SVM), Osteoporosis, Co-occurrence matrix, Run-length matrix.*

Introduction

Osteoporosis is nowadays a global health issue of humans, which affects especially the health condition and life quality of senior citizens. About one third of elderly people in their 60s-70s across the world are suffering from osteoporosis. Thus, it is on the list of the top five serious diseases made by the international medical field. Chinese patients having osteoporosis are sharply increasing along with the acceleration of China's population aging. Accordingly, early diagnosis and prevention of osteoporosis has become significantly important.

Bone histomorphometry is widely applied in osteoporosis research in common medical experiments, although this process is complicated and takes a long period from specimen making to measurement, image analysis and process techniques. In contrast, it is seldom used in osteoporosis related issues, like texture analysis [7] or osteoporosis related factors [1, 3], regardless of its extensive application in many fields of medical imaging. In this paper, image

texture analysis based on statistical analysis and a classification based on a Support Vector Machine (SVM) were introduced. The bone tissue sections were observed directly under a microscope and images were taken, of which a texture analysis was made in the regions of interest (ROIs, namely, the bone trabecular) to test the difference of the characteristic parameters; then the parameters with significant difference were chosen as the feature variables, of which classification recognition was made with the SVM method. Research was carried out with linear, multi-kernel, RBF and sigmoid kernel functions, and finally, leave-one-out cross-validation was applied to prove the accuracy of the classification results. The purpose of this paper is to develop a new method for texture analysis research and apply this result in clinical osteoporosis diagnosis in accordance with medical images.

Materials and methods

Animals for the experiment and the feeding conditions

Twenty 3-month-old female SD rats, with an average weight of 250.1 g, were used as experimental animals. They were divided into 2 groups: (1) SHAM group: sham rats, lavaged with 5 ml (kg·d) physiological saline; (2) OVX group: ovariectomized rats, lavaged with 5 ml (kg·d) physiological saline. Each group consisted of 10 rats, and the experiment lasted 90 days. Feeding conditions were as follows: temperature between 24 °C ~ 28 °C, humidity between 50% ~ 60%; all animals were kept in an exclusive room, two in one cage, with the padding materials changed on alternate days; they were fed on standard feedstuff supplied by our animal center, and weighed once a week, and they took distilled water. The animal study proposal was approved by the Institutional Animal Care and Use Committee (IACUC) of the Guangdong Medical College. All the experimental procedures were performed in accordance with the Regulations for the Administration of Affairs Concerning Experimental Animals approved by the State Council of People's Republic of China.

Specimen processing and making method

25 mg/kg totomycin and 5 mg/kg calcein were hypoed to all the rats for 13 and 14 days, as well as 3 and 4 days before their death respectively, and the two fluorescence labels were made with a gap of 10 days. After the experiment, they were given an intraperitoneal injection of 3% amobarbital sodium (1.5 ml/kg). Next, all blood in the ventriculus dexter was drawn (to reduce the red blood cell number in the marrow so as to avoid interference and to guarantee better observation and analysis), and then undecalcified bone sections were made in the upper shankbones. A specimen could be made to the sections in 5 μm (thin) or 9 μm (thick), the former one required the use of toluidine blue, and the latter one could be sealed directly. Afterwards, a bone morphometry static test was made to the sections and the parameters [6] could be obtained according to the expressions.

Facilities and software

The facilities and software used included: a carbonized tungsten steel knife and a LEICA2155 Hard tissue sheeter manufactured by LEICA, located in Germany, an automatic digital image analyzer including a light microscope and a fluorescence microscope (Nikon, Japan), bone morphometric measurement software (KSS Scientific Consultants, UT USA) and texture analysis software (Mazda).

Texture analysis method

The authors firstly observed and photographed the thick bone tissue sections under a microscope (magnified 4 times) then made a texture analysis of the images with Mazda and chose the ROI area to test the difference between the texture parameters. Next, the parameters

with significant differences were chosen as the feature variables, on which classification recognition was made with a SVM, a research was made with linear, polynomial, RBF and sigmoid kernel functions, and finally, leave-one-out cross-validation was applied to prove its accuracy.

Results

Abstraction of texture characteristics

Texture analysis technology studies the change and the distribution rules of the grayscales of the images. It can abstract image characteristics and find digital features that describe the texture with image processing techniques to get quantitative descriptions for image analysis. The various statistics of a co-occurrence matrix and a run-length matrix in partial areas of the images are the digital texture features commonly used. Texture analysis, as a key measure for feature abstraction and classified recognition, can be used to describe the component distribution situation of any substance, and obtain important information of the object in the image, since texture represents the structure of an object.

In medical diagnosis, the distribution of organic tissues in large-scale can be considered as a texture phenomenon, and there is an obvious difference in size and distribution of the textures of normal and pathologic tissues. Shape and texture are two representative visual measuring means in medical image with revelatory significance in diagnosis. The examination of medical images generally requires an explanation of the appearance of tissues, such as smoothness, particle size, regularity and homogeneity, etc., which often closely correlates to the partial greyscale change of an image; thus, a medical image can be analyzed and researched through texture measurement.

In this paper, the bone tissue sections were observed directly under a microscope and images were taken, of which a texture analysis was made in the ROIs, shown in Fig. 1.

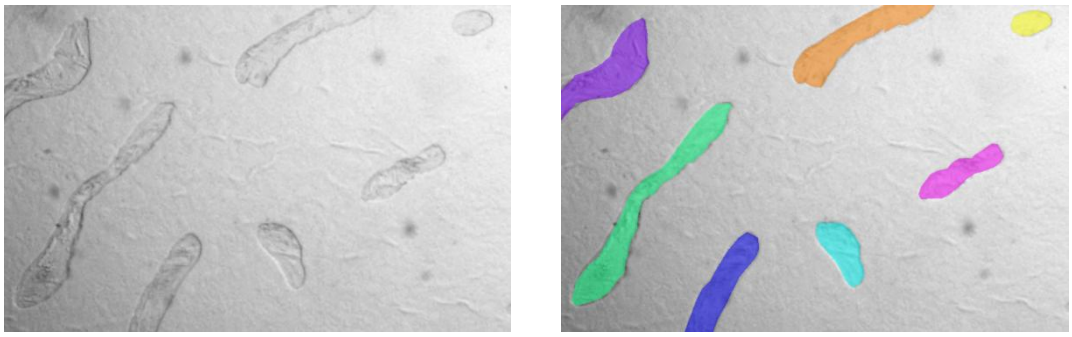

(a) The original photo (magnified 4 times) (b) The photo with ROIs

Fig. 1 The original photo and the photo with ROIs

The researcher abstracted texture features from the ROIs on the directions of 0°, 45°, 90° and 135° with a co-occurrence matrix and a run-length matrix. The feature parameters obtained are shown in Table 1.

Table 1. Texture features used in the analysis

Feature parameters	Formula
Angular second moment energy (AngScMom)	$\sum_{i=1}^{Ng}\sum_{j=1}^{Ng} p(i,j)^2$
Contrast	$\sum_{n=0}^{Ng-1} n^2 \sum_{\substack{i=1 \\ \lvert i-j\rvert=n}}^{Ng}\sum_{j=1}^{Ng} p(i,j)$
Correlation (Correlat)	$\frac{\sum_{i=1}^{Ng}\sum_{j=1}^{Ng} ijp(i,j) - \mu_x\mu_y}{\sigma_x\sigma_y}$
Sum of squares (SumOfSqs)	$i = \sum_{i=1}^{N_g}\sum_{j=1}^{N_g}(i-\mu_x)^2 p(i,j)$
Inverse difference moment (InvDfMom)	$\sum_{i=1}^{Ng}\sum_{j=1}^{Ng}\frac{1}{1+(i-j)^2} p(i,j)$
Sum average (SumAverg)	$\sum_{i=1}^{2Ng} ip_{x+y}(i)$
Sum variance (SumVarnc)	$\sum_{i=1}^{2N_g}(i-SumAverg)^2 p_{x+y}(i)$
Entropy	$-\sum_{i=1}^{Ng}\sum_{j=1}^{Ng} p(i,j)\log(p(i,j))$
Sum entropy (SumEntrp)	$-\sum_{i=1}^{2Ng} p_{x+y}(i)\log(p_{x+y}(i))$
Difference variance (DifVarnc)	$\sum_{i=1}^{Ng-1}(i-\mu_{x-y})^2 p_{x-y}(i)$
Difference entropy (DifEntrp)	$-\sum_{i=1}^{Ng} p_{x-y}(i)\log(p_{x-y}(i))$
Run-length nonuniformity (RLNonUni)	$(\sum_{j=1}^{Nr}(\sum_{i=1}^{Ng} p(i,j))^2)/C$
Grey-level nonuniformity (GLevNonU)	$(\sum_{i=1}^{Ng}(\sum_{j=1}^{Nr} p(i,j))^2)/C$
Long run emphasis (LngREmph)	$(\sum_{i=1}^{Ng}\sum_{j=1}^{Nr} j^2 p(i,j))/C$
Short run emphasis (ShrtREmp)	$(\sum_{i=1}^{Ng}\sum_{j=1}^{Nr}\frac{p(i,j)}{j^2})/C$

Note: $p(i, j)$ refers to the times of j shown when the grayscale is i, Ng is the grayscale number, and Nr is the run length.

The weighted average texture parameters of the four directions on ROIs calculated included the texture parameter data of both SHAM and OVX. Then the parameters with significant differences were determined with two separate sample tests as the data base for the further classification recognition.

SVM method and leave-one-out cross-validation

SMV method

A SVM is suitable for the solution of binary model recognition issues, especially for small samples, non-linear and high dimensional models.

Take linearly separable problems as an example, the basic thinking of a SVM is shown in Fig. 2, in which the two kinds of points refer to different training samples, many decision planes can correctly divide data, while the SVM collects all training data to find the decision plane with the largest class interval, namely the optimal separating hyperplane (the full line in Fig. 2), which makes the nearest point of all kinds of data divided by it remain at the largest distance from it. We do not have to consider all points, but only need to make sure that the optimal separating hyperplane found can make the training sample point that is the nearest to it remain at the largest distance from it. To get the biggest classification interval means to maintain the smallest confidence region, or the smallest actual risk. If this optimal separating hyperplane is found, then the classifier is the one with the biggest interval.

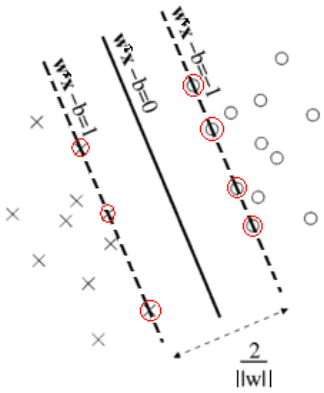

Fig. 2 Optimal separating hyperplane

In the following part, the authors will discuss the above statement.

Assume x_i, $i = 1, 2, 3, \ldots, N$ is the feature vector of the training set X, from w_1,w_2, and assume they are linearly separable. The purpose is to design a hyperplane to correctly classify all the training vectors. The equation of the hyperplane is as follows:

$$g(x) = w^{\mathrm{T}}x + b = 0$$

It is obvious that the hyperplane is not unique, and determined by w and b. We know that the vector w is perpendicular to the classification hyperplane, in accordance with geometry. Shifting b is added to increase the interval.

Since it is required that the interval be the biggest, we need to know the support vector (the points circled in Fig. 2) and the the hyperplane that is parallel and the nearest to the optimal separating hyperplane. Those parallel hyperplanes can be expressed with the following equations (since w is a normal vector of a hyperplane with an unfixed length, it is a variable, 1 and –1 are both constants set to make the computation easier, they can be any other constants that are opposite):

$$w^{\mathrm{T}}x + b = 1, \quad w^{\mathrm{T}}x + b = -1$$

As it is assumed that the training data is linearly separable, two hyperplanes with the biggest distance and no sample point between them can be found. Then we can calculate the gap between them, which is $2/\|\boldsymbol{w}\|$; thus, we should minimize $\|\boldsymbol{w}\|$. In the meantime, in order to guarantee that all sample data points are not in the interval, i must meet either of the following conditions:

$w^{\mathrm{T}}x_i + b \geq 1$ or $w^{\mathrm{T}}x_i + b \leq -1$

For each x_i, y_i is used to express the marker of the corresponding kind. Accordingly, the optimal separating hyperplane can be found by solving the following quadratic problems:

$$min \frac{1}{2}\|w\|^2$$

$$s.t.\ \ y_i(w^{\mathrm{T}}x_i + b) - 1 \geq 0, \quad i = 1, 2, ..., N$$

While solving the nonlinear problems, we can map the samples to a high dimensional space and then solve them with the same method. In this way, the optimal separating hyperplane is changed to an optimal separating hyperplane in a higher dimensional space. Assume that the mapping is Φ; then the classification equation is changed to:

$$d(x) = (w^*)^{\mathrm{T}} \Phi(x) + b^* = \sum_i \alpha_i^* y_i \Phi^{\mathrm{T}}(x_i)\Phi(x) + b^*$$

It can be found that only the inner product of the shifting high dimension $\Phi^{\mathrm{T}}(x_i)\ \Phi(x_j)$ is involved, and such a function can also be considered as a kernel function:

$\ker(x, x_i) = \Phi^{\mathrm{T}}(x_i)\ \Phi(x)$

According to the Hilbert-Schimidt theory, the kernel function is equivalent to the inner product of a space, provided that it meets the Mercer condition [4]. Model recognition often contains the following kinds of kernel functions:

polynomial kernel function: $\ker(x, x_i) = (x^{\mathrm{T}}x_i + 1)^q$

RBF kernel function: $\ker(x, x_i) = \exp\left(-\frac{|x - x_i|^2}{\sigma^2}\right)$

sigmoid kernel function: $\ker(x, x_i) = \tanh[\gamma(x^{\mathrm{T}}x_i) - \theta]$

Considering that there was only a small quantity of samples, in this paper, linear, polynomial, RBD and sigmoid kernel functions were used in the research and leave-one-out cross-validation was applied to prove its accuracy.

Leave-one-out cross-validation (LOOCV)

Cross-validation (CV), or circle validation, is a statistical analysis method used to validate the performance of a classifier. Pioneered by Seymour Geisser, the theory of CV plays an important role in testing hypotheses suggested by the data, especially for the cases when the subsequent samples are dangerous, expensive or limited.

The main idea of CV is dividing the original data into a training set and a validation set, then training the classifier with the training set, and testing the model obtained from the training with the validation set, from which the results are considered as the performance index for classifier evaluation.

LOOCV is a form of CV. Assume that the primary data has N samples, LOOCV considers every single sample as a validation set and the other $N - 1$ samples as the training set, so it will get N models after the whole course is finished. The average classification accuracy of the final validation set of the N models is regarded as the performance index of the LOOCV classifier. LOOCV has two disadvantages: first, in each round, nearly all the samples are considered as a training model, thus, it is similar to the distribution of the original data and the evaluation result is more accurate; second, there are no random factors that can affect the experimental data during the experiment, and, accordingly, the experimental process is reproducible.

Due to the limited samples, in this paper, linear kernel, polynomial kernel, RBF kernel and sigmoid kernel of a SVM were adopted for classification study and LOOCV was introduced to validate classification accuracy.

Recognition results of osteoporosis experiment based on texture features and SVM classifier

The texture parameters with significant differences between SHAM and OVX after *T*-test are shown in Table 2 as follows:

Table 2. Texture features with significant differences between the groups

	SHAM group	**OVX group**
AngScMom	0.07±0.03	0.13±0.05
Contrast	1.46±0.45	0.6±0.17
SumOfSqs	8.71±7.21	2.82±1.65
InvDfMom	0.72±0.05	0.79±0.03
SumVarnc	33.39±28.69	10.67±6.54
SumEntrp	1.22±0.15	0.98±0.15
Entropy	1.51±0.21	1.16±0.18
DifVarnc	0.92±0.24	0.40±0.09
DifEntrp	0.47±0.05	0.35±0.04
RLNonUni	9244.74±10921	1692.33±1511.09
GLevNonU	1970.67±1134.96	892.01±625.32
LngREmph	9.33±3.31	14.89±4.62
ShrtREmp	0.63±0.05	0.52±0.05

From the table above, it can be seen that AngScMom, InvDfMom, and DifEntrp are higher in the SHAM group that those in the OVX, while in contrast, SumVarnc, Entropy, SumEntrp, DifVarnc, DifEntrp, RLNonUni, GLevNonU, ShrtREmp are higher than those in the OVX. On the basis of the texture parameters with differences in Table 2, classification recognition was made to the samples with SVM; linear, polynomial, RBF and sigmoid kernel functions were applied, and then LOOCV was made to prove their accuracy, and the results are shown in Table 3.

From Table 3 and Fig. 3, it can be found that the classification obtained with the linear kernel function provides the highest accuracy for both the SHAM and the OVX groups, as well as the highest average accuracy. Therefore, the linear classifier is the best option for this experiment.

Table 3. Recognition accuracy of four kinds of kernel functions

	Linear	Polynomial	RBF	Sigmoid
SHAM	93.75	100	87.50	87.50
OVX	90.91	36.37	90.91	81.82
Average accuracy	92.59	74.07	88.89	85.19

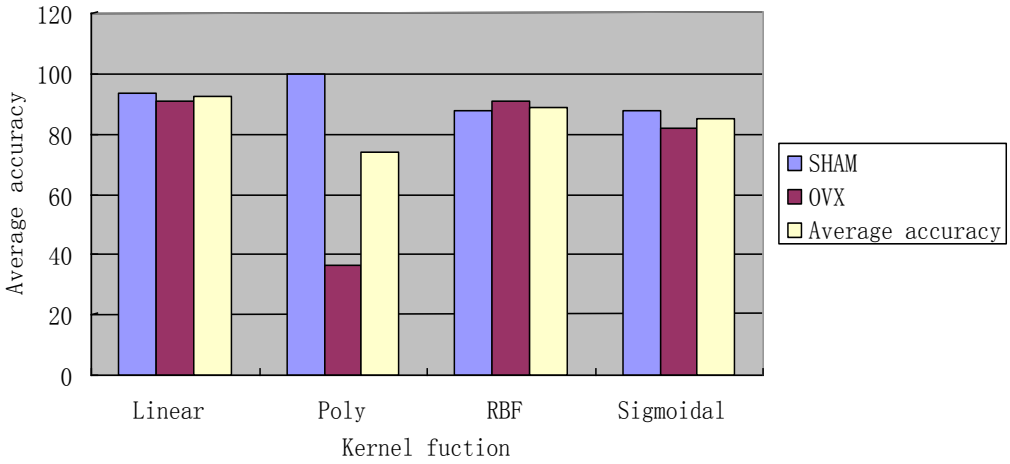

Fig. 3 Recognition accuracy of four kinds of kernel functions

Recognition results of osteoporosis experiment based on texture features and SVM classification

The texture parameters with significant differences between SHAM and OVX after the *T*-test are shown in Table 4.

Table 4. Texture features with significant differences between the groups

	SHAM group	OVX group
AngScMom	0.07±0.03	0.13±0.05
Contrast	1.46±0.45	0.6±0.17
SumOfSqs	8.71±7.21	2.82±1.65
InvDfMom	0.72±0.05	0.79±0.03
SumVarnc	33.39±28.69	10.67±6.54
SumEntrp	1.22±0.15	0.98±0.15
Entropy	1.51±0.21	1.16±0.18
DifVarnc	0.92±0.24	0.40±0.09
DifEntrp	0.47±0.05	0.35±0.04
RLNonUni	9244.74±10921	1692.33±1511.09
GLevNonU	1970.67±1134.96	892.01±625.32
LngREmph	9.33±3.31	14.89±4.62
ShrtREmp	0.63±0.05	0.52±0.05

From the table above, it can be seen that AngScMom, InvDfMom, and DifEntrp are lower in the SHAM group that those in the OVX, while, in contrast, SumVarnc, Entropy, SumEntrp,

DifVarnc, DifEntrp, RLNonUni, GLevNonU, ShrtREmp are higher than those in the OVX. On the basis of the texture parameters with differences in Table 2, classification recognition was made to the samples with SVM; linear, polynomial, RBF and Sigmoid kernel functions were applied, and then LOOCV was made to prove their accuracy. The results are shown in Table 5.

Table 5. Recognition accuracy of the four kinds of kernel functions

	Linear	**Polynomial**	**RBF**	**Sigmoid**
SHAM	93.75	100	87.50	87.50
OVX	90.91	36.37	90.91	81.82
Average accuracy	92.59	74.07	88.89	85.19

From Table 5, it can be found that the classification obtained with the linear kernel function provides the highest accuracy for both the SHAM and the OVX groups, as well the highest average accuracy. Therefore, the linear classifier is the best option for this experiment.

Certainly, recognition accuracy is admittedly the most important, but the error possibility should also be considered, since diagnosis errors can result in negative consequences for the patients. For this reason, we have calculated the error rates of the four kernel functions. (1) recognized as the SHAM group, when it is actually the OVX group; (2) recognized as the OVX group, when it is actually the SHAM group. Meanwhile, we also calculated the overall error rate of the four functions, namely, the ratio of mistakenly recognized images to the total image number. Please, refer to the Table 6.

Table 6. Error rates of recognition based on the four kernel functions (%)

	Linear	**Polynomial**	**RBF**	**Sigmoid**
(1)	6.25	30.43	6.67	12.50
(2)	9.09	0.00	16.67	18.18
Overall error rate	7.41	25.93	11.11	14.81

All in all, the SVM based on Linear provides the highest accuracy rate and the lowest error rate in recognition.

Discussion and conclusion

Traditional bone histomorphometry is the gold standard of the quantitative analysis of bone microstructure, and the major basis of the diagnosis of osteoporosis and its efficacy criterions. It builds its foundation on stereology and calculates the related parameters of microstructure with 2D images, but ignores the different characteristics and the three-dimensional structure of bone trabecula.

Noninvasive computed tomography, which can precisely describe the 3D distribution and morphological features of the structure, conquers the limits of 2D tissue slices, and can show all the differences of the 3D structural parameters. However, higher spatial resolution means a smaller probe volume, and an amplification system of high sensitivity and low noise, which restricts the application of micro CT in humans and big animals.

In a previous study, we found that the bone tissue image in normal rats and the ovariectomized osteoporosis rats can be distinguished through texture analysis at the magnification of 10 times [5]. In this paper, under the same technical parameters, adopting

low power lens (4 times) and choosing ROIs greatly reduced workload. The effectiveness of texture analysis, however, still needs further study.

The test was made after the texture parameters were abstracted from the SHAM and the OVX groups and it was found out that there was a significant difference between the two sets of data ($p < 0.05$, and the same conclusion can be reached even if $p = 0.001$). The result shows that texture analysis can distinguish between SHAM and OVX, and it has provided a scientific basis for the application of texture analysis in the early clinical diagnosis and prevention of osteoporosis.

Texture analysis technology studies the change and distribution rules of the grayscale of images; thus, texture features can reflect the microscopic pathological changes that are invisible to the naked eye. Bone trabecular, as the basic unit to describe osteoporosis, was chosen as the object of this analysis. Although it may be caused by many reasons, osteoporosis is the unbalanced calcium-phosphorus metabolism of a human body and the reduction of bone density due to the defection of coupling in bone absorption and formation during the bone metabolism. It will then lead to a change of the grayscale of the images and texture characteristics.

In accordance with the meanings represented by the texture parameters and the data in Table 2, it can be seen that the value of "the angular second moment energy" is higher when the image is finer and more uniform, since it shows the uniformity of the grayscale of the images distribution and texture size. Also, the value of "the inverse difference moment" varies inversely with the regularity of the texture, considering that it expresses texture regularity, and the value is proportional to the quantity of rough textures. As for "the long run emphasis", its value is higher when the image is finer and more uniform. Based on the results above, it can be concluded that the images of SHAM are finer and more complex than those of OVX. "Contrast" represents image resolution and texture intensity; thus, a higher contrast value refers to a better contrast and texture effect. "Sum variance" shows the changing period of texture, the value varies with different image textures and can be considered as an important index to distinguish textures. "Difference variance" is the variance of the nearby grayscale difference, whereas a more obvious contrast leads to a higher difference variance value. "Entropy", "sum entropy" and "difference entropy" all express the information content of the image. They measure the randomness of the image content and the texture complexity; when the image is very complex, entropy value reaches the highest and the other two values will be higher too. "Grey-level nonuniformity" describes the similarity of the greyscales of the images, similar greyscale values of the image lead to a lower grey-level nonuniformity value. "Short run emphasis" shows the distribution condition of the short run, and the value is proportional to the number of fine textures in the image. These results have further proven that SHAM shows a higher contrast of the texture units, a higher texture complexity, a lower similarity in grey-scale values regarding the entire image, and finer textures compared to OVX. This conclusion is consistent with the basic fact that the image directly reflects the decreased bone density and the vague bone structure in osteoporosis [2]. For this reason, image texture analysis can be applied instead of the traditional method to recognize and diagnose osteoporosis. The application of texture analysis in clinical imaging can help fast diagnose osteoporosis and start the treatment earlier.

Furthermore, the SVM method shows a high recognition accuracy and robustness for a small quantity of samples. It is particularly significant for diagnosis results in medical experiments or when clinical cases are limited. However, its application in osteoporosis diagnosis when

the sample quantity is large and other osteoporosis issues are involved needs further verification.

The results and discussion may be combined into a common section or presented separately. They may also be broken into subsections with short, informative headings.

Acknowledgements

We acknowledged the Guangdong Science and Technology Project, China (No. 2010B031600291, 2010A040200005), and Zhanjiang Municipal Science and Technology Challenging Project, China (No. 2011C3107016) for financial support.

References

1. Karunanithi R., S. Ganesan, T. M. R. Panicker, M. P. Korath, K. Jagadeesan (2007). Assessment of Bone Mineral Density by DXA and the Trabecular Microarchitecture of the Calcaneum by Texture Analysis in Pre- and Postmenopausal Women in the Evaluation of Osteoporosis, Journal of Medical Physics, 32(4), 161-168.
2. Li Q., T. Wu, C. Li, et al. (2001). The Osteoporosis Experimental Animal Study, Bone Histomorphometry, Sichuan University Press, 23-44, (in Chinese).
3. Mallard F., B. Bouvard, P. Mercier, P. Bizot, P. Cronier, D. Chappard (2013). Trabecular Microarchitecture in Established Osteoporosis: Relationship between Vertebrae, Distal Radius and Calcaneus by X-ray Imaging Texture Analysis, Orthopaedics & Traumatology: Surgery & Research, 99(1), 52-59.
4. Theodoridis S., K. Koutroumbas (2010). Pattern Recognition, 4th Ed., Academic Press, Elsevier.
5. Wu T., J. Cai (2014). Osteoporosis Measurement based on Texture Analysis, Chinese Journal of Osteoporosis, 20(7), 10-14, (in Chinese).
6. Wu T., J. Liao, S. Liu, Y. Chen, L. Huang, W. Chen (2012). Effects of XianZhenGuBao on Lumbar Vertebrae in Ovariectomized Rats by Bone Histomorphometry, Guangdong Medical Journal, 13, 1883-1886, (in Chinese).
7. Yang X., D. Zhang, D. Jiang (2001). A Study on Quantitative Assessment of Osteoporosis Based on Texture Analysis, Journal of Biomedical Engineering, 18(3), 403-407, (in Chinese).

Jie Cai, M.Sc.
E-mail: caijie513@163.com

Jie Cai is a lecturer. She had her major in Applied Mathematics. Now she is engaged in the researches on medical data mining and medical image analysis and processing.

Assoc. Prof. Tian-Xiu Wu, M.Sc.
E-mail: wutianxiu2005@163.com

Tian-Xiu Wu is an Associate Professor and a Postgraduate Supervisor. Her areas of expertise are bone biology and osteoporosis.

Assoc. Prof. Ke Zhou, M.Sc.
E-mail: kitty@gdmc.edu.cn

Ke Zhou is an Associate Professor. She had her major in Computer Application. Now she is engaged in the researches on medical data mining and medical image analysis and processing.

Assoc. Prof. Wende Li
E-mail: gdmcli@qq.com

Wende Li is an Associate Professor, a Postgraduate Supervisor and a Postdoctoral Research Fellow at Massachusetts General Hospital, Harvard Medical School. His areas of expertise are 1) building the express FAT1 gene Alzheimer's disease model, and 2) studying the biology of MicroRNA378 in mice model. He is currently leading one general project of the National Natural Science Foundation of China and one general project of the Natural Science Foundation of Guangdong. Also as a principle investigator he has participated in two National Cancer Institute/Federal Share projects, USA. His most recently research results were published in the Radiotherapy and Oncology journal.